Phase-Shifting Multi-Wavelength Dynamic Interferometer

Michael B. North-Morris, James E. Millerd, Neal J. Brock and John B. Hayes
4D Technology Corporation, Tucson, AZ

ABSTRACT

The benefits of using two-wavelength measurements to extend the dynamic range of an interferometric measurement are well known. We present a new multi-wavelength interferometer that uses two successive single frame measurements obtained rapidly in time to significantly reduce sensitivity to vibration. At each wavelength, four phase-shifted interferograms are captured in a single image. The total acquisition time for both wavelengths is 100 microseconds, over three orders of magnitude shorter than conventional interferometers. Consequently, the measurements do not suffer from the fringe contrast reduction and measurement errors that plague temporal phase-shifting interferometers in the presence of vibration. In this paper we will discuss the basic operating principle of the interferometer, analyze its performance and show some interesting measurements.

Keywords: Interferometry, Surface Measurement, Multiple Wavelength

1. INTRODUCTION

The testing of segmented primary telescope mirrors requires the measurement of potentially large step discontinuities between segments (millimeters) and at the same time requires high resolution (nanometers) to verify surface figure of the elements. In addition, the difficulty of vibrationally isolating large meter-class optics requires a measurement technique that is highly immune to vibration. Contact profiling and broadband vertical scanning techniques are capable of measuring the discontinuities with the required accuracy in controlled environments. However, the relatively long acquisition cycle precludes the use of these methods in the presence of vibrations. Two-wavelength interferometry can also provide the ability to measure large discontinuities with high resolution[1]. Although, combined with traditional phase-shifting techniques a two-wavelength measurement can be acquired in a fraction of the time of the profiling techniques, the acquisition time is too slow to provide vibration immunity. The multi-wavelength interferometer presented here combines two-wavelength capability with spatial phase shifting to overcome the speed limitations of traditional phase-shifting interferometry. The system achieves a measurement range of millimeters and a resolution of a few nanometers with an acquisition time of less than 100 microseconds. In addition, there are multiple wavelengths available that allow the dynamic range of the two-wavelength measurement to be adjusted making it possible to remove phase ambiguities all the way down to the fundamental wavelength.

A variety of methods for spatial phase-shifting have been developed over the years. The most common are the use of multiple cameras to detect multiple interferograms[2,3], the use of diffractive elements to simultaneously image three or more images onto a single CCD[4,5] and the use tilt to introduce a spatial carrier frequency to the pattern[6]. The multiple camera approach tends to be expensive and difficult to implement, the diffraction approach only works over a limited wavelength range due to dispersion and the spatial carrier approach is difficult to implement at two different wavelengths simultaneously.

The spatial phase-shifting used here does not fall directly into any of the above categories. The four phase-shifted frames are simultaneously captured by placing a pixelated phase-mask directly in front of the CCD that introduces a unique phase-shift at each pixel. In addition, to the achromatic design of the phase mask, the pixelated approach to phase-shifting does not suffer from dispersion making it ideal for multi-wavelength applications. Pixelated phase shifting has the following advantages:
1) A true common path arrangement permits the of broadband or white light
2) Extremely compact design
3) Achromatic over a very wide range
4) Fixed spatial interference pattern results in fast processing

2. MEASUREMENT TECHNIQUE

2.1 Simultaneous phase-shift measurement

At the heart of the interferometer is a new achromatic spatial phase-shifting interferometer in which four phase-shifted interferograms are simultaneously generated on a single detector array. The optical layout of the interferometer is shown in figure 1. The basic configuration is a Twyman-Green. An expanded and collimated beam from the source module is incident on a zero-order half-wave birefringent plate that is used to rotate the input polarization. By rotating the polarization angle, the power split between the orthogonally polarized test and reference arms of the interferometer continuously. The polarizing beam splitter splits the test and reference arms into orthogonal polarizations and the zero-order quarter-wave plates are used in double pass to rotate the orientation of the polarization in the test and reference arms by ninety degrees. The test arm of the interferometer is coupled to the test mirror by a diverging optic when measuring a concave mirror, or is collimated by a telescope for measuring a plane mirror. On the second pass the polarizing beam splitter recombines the test and reference beams. The imaging optics image the test surface onto the CCD. Mounted directly in front of the CCD is a pixelated phase mask that encodes a high spatial frequency interference pattern on the two orthogonally polarized collinear test and reference beams. The phase mask is designed to have a one-to-one pixel correspondence with the CCD, that is to say that each pixel on the CCD receives and individually phase-shifted signal. The phase mask has four unique phase shifts (ABCD) and is patterned so that every pixel is in quadrature with its neighbors. The phase-difference between the test and reference arms is obtained by using an N-bucket algorithm or by spatial convolution. The phase-mask is designed to operate over a wide spectral range making it ideal for multiple-wavelength applications.
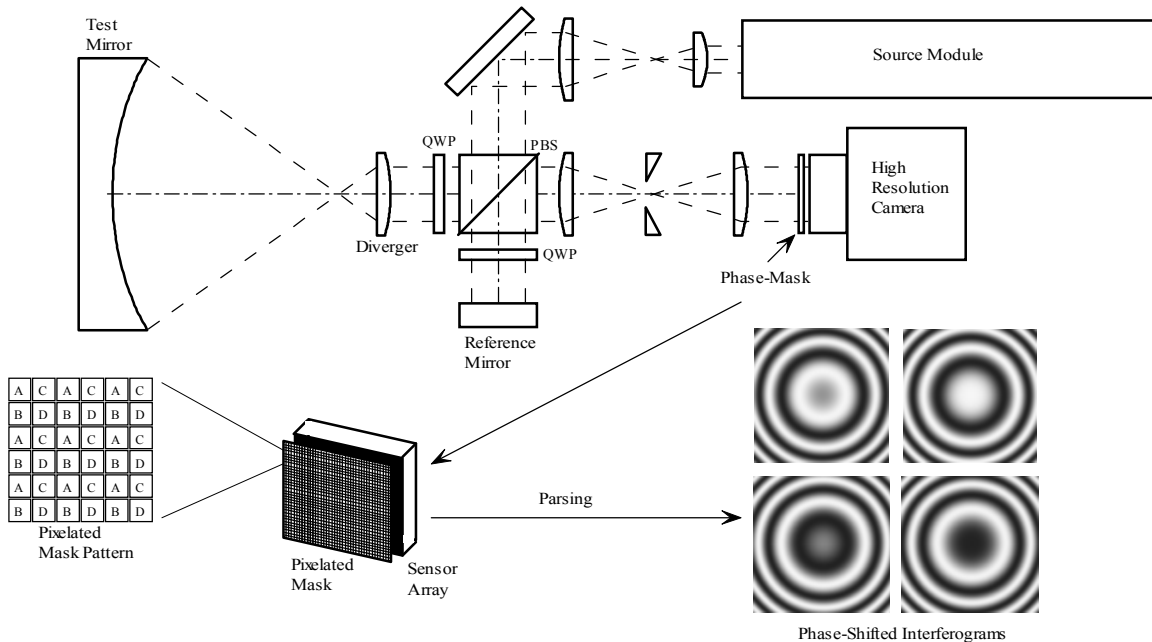

Figure 1: Spatial Phase-Shifting

Some of the advantages for multi-wavelength applications of the pixelated approach to phase-shifting are that it is common path, achromatic over a very wide range of wavelengths and the spatial interference pattern is fixed with wavelength.

2.2 Source coupling and switching

In addition to simultaneous acquisition of the four phase-shifted interferograms afforded by spatial phase-shifting, fast switching and short integration times are desirable to avoid a reduction in fringe contrast and minimize changes in the

phase between the two individual wavelength measurements in the presence of vibrations. High-speed switching and relatively efficient coupling of the three laser sources is accomplished in the source module. Three sources, two fixed in wavelength and one tunable, are coupled into the interferometer using a combination of polarizing beam splitters, a half-wave plate, acousto-optic light modulators and a polarizer as shown in figure 2. The polarizing beam splitters and half-wave plates provide relatively efficient coupling of the three sources. The orthogonally polarized TLS and 660nm lasers are folded into the optical path of the interferometer by a polarizing beam splitter and a half waveplate rotates the polarization of each to maximize the throughput through the second polarizing beam splitter. The fundamental source (637nm) is folded into the optical path by the second polarizing beam splitter and is orthogonally polarized with the other two sources at that point. Finally, the polarizer is rotated to balance the throughput of the two orthogonally polarized components providing a constant state of input polarization to the interferometer. When compared with coupling without taking advantage of polarization this approach offers a 50% improvement in throughput. The AOMs supply high speed switching between sources. The AOMs are capable of switching between sources in a few microseconds. Taking into account the fluence at the CCD, the camera frame transfer capabilities and sensitivity, and the switching capabilities of the AOMs the resulting acquisition time is less than 100μs for a two-wavelength measurement.
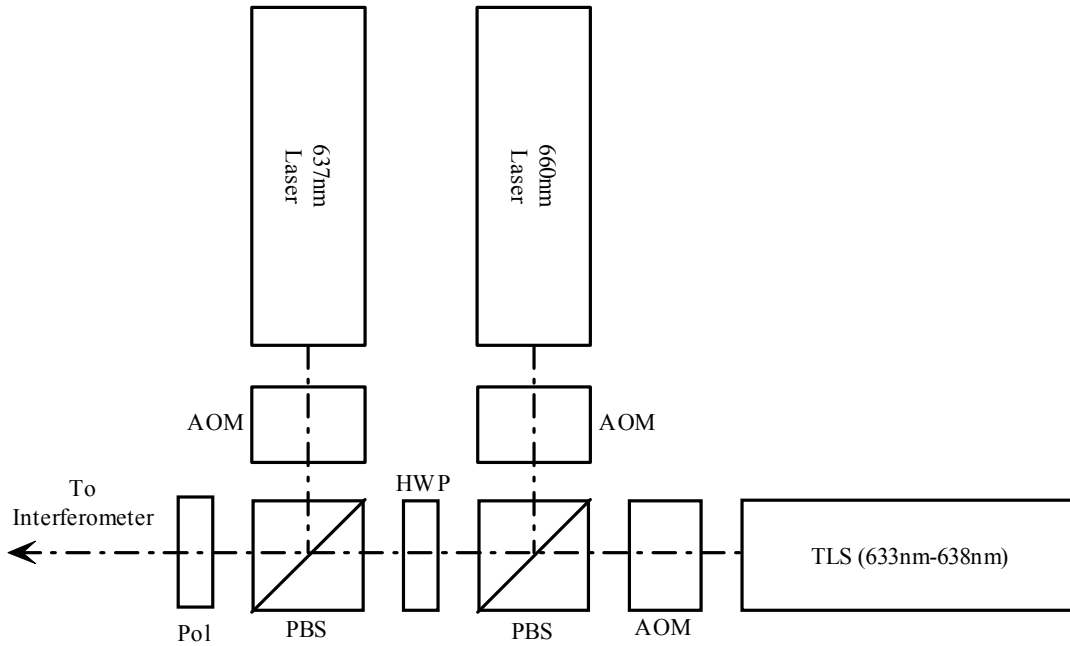

Figure 2: Source Coupling and Switching

2.3 Measurement subtraction

Synthetic-wavelength measurements are made by capturing two measurements at different wavelengths and subtracting the phase. The measured difference in surface height is given by

$$\Delta z(x,y) = \frac{\Delta f_s(x,y)}{4 \cdot p} \cdot l_s \tag{2.1}$$

$$where, \ \Delta f_s(x,y) = \Delta f_1(x,y) - \Delta f_2(x,y) \ and \ l_s = \frac{l_1 \cdot l_2}{|l_1 - l_2|}$$

Δf_s and l_s are the synthetic phase and wavelength respectively, l_1 and l_2 are the two wavelengths used to make the measurement and, Δf_1 and Δf_2 are the corresponding measured phases for the two single wavelength measurements.

The phase subtraction can be made directly in the phase domain as shown above or it can be performed in the interferogram domain for reduced sensitivity to random irradiance fluctuations, facilitating the ability to measure diffuse as well as specular surfaces. The algorithm for the interferogram subtraction can be derived by applying the following trigonometric identity to the phase subtraction.

$$Tan(a-b) = \frac{Tan(a) - Tan(b)}{1 + Tan(a) \cdot Tan(b)} \qquad (2.2)$$

The resulting algorithm is

$$\Delta f_s(x,y) = ArcTan\left(\frac{X(x,y)}{Y(x,y)}\right) \qquad (2.3)$$

where .

$$X(x,y) = [D_1(x,y) - B_1(x,y)][A_2(x,y) - C_2(x,y)] - [A_1(x,y) - C_1(x,y)][D_2(x,y) - B_2(x,y)]$$

$$Y(x,y) = [A_2(x,y) - C_2(x,y)][A_1(x,y) - C_1(x,y)] + [D_1(x,y) - B_1(x,y)][D_2(x,y) - B_2(x,y)]$$

A_1, B_1, C_1, D_1 are the phase-shifted interferograms at l_1, and A_2, B_2, C_2, D_2 are the phase-shifted interferograms at l_2.

Noise in the measurement can be significantly reduced using a weighted spatial average over neighboring pixels. This can be accomplished by:

$$\Delta f_s(x,y) = ArcTan\left(\frac{\sum\limits_{x,y \in d} X(x,y)}{\sum\limits_{x,y \in d} Y(x,y)}\right), \qquad (2.4)$$

where the sums are performed over the range of d nearest neighbors. Because of the modulo $2p$ behavior of the arctangent function, the range is wrapped (ambiguous) beyond the so-called synthetic wavelength. Any number of well-known processes of spatial phase unwrapping can be used to remove the discontinuous steps and perform quantitative analysis of the interferograms.

3. SOURCE REQUIREMENTS

3.1 Synthetic wavelength range
The useable synthetic wavelength range of the multi-wavelength interferometer is governed by the source wavelengths available and the uncertainty of determining the relative wavelengths. The sensitivity to wavelength uncertainty increases with synthetic wavelength. Figure 3 graphically shows the synthetic wavelength range for this particular interferometer. The broadest range of synthetic wavelengths is produced by using the fundamental source and the TLS which overlap in wavelength. The upper end of the synthetic wavelength range is limited to 10 mm by the uncertainty of the source wavelengths. The lower end of the range is limited to 115 microns due to the wavelength range of the tunable source (5nm). There is a region between 3mm and 7mm in synthetic wavelength that requires the TLS to tune over a range too large for the accurate piezo-electric transducer and the wavelength uncertainty of course tuning the DC motor becomes large. This small range of synthetic wavelength is not recommended for operation; however, this does not present a serious limitation for most practical situations. The third laser source (fixed 660nm) was added to help bridge the gap between the lowest tunable synthetic wavelength and the fundamental wavelength. Combining measurements made with the two fixed sources we can measure at a synthetic wavelength of approximately 18 microns. Without this intermediate step the synthetic wavelength measurements would require an accuracy of approximately 1/1000th of a wave to reliably correct the phase ambiguities at the fundamental wavelength. Adding the 18 micron synthetic wavelength reduces the required accuracy to approximately 1/60th of a wave.
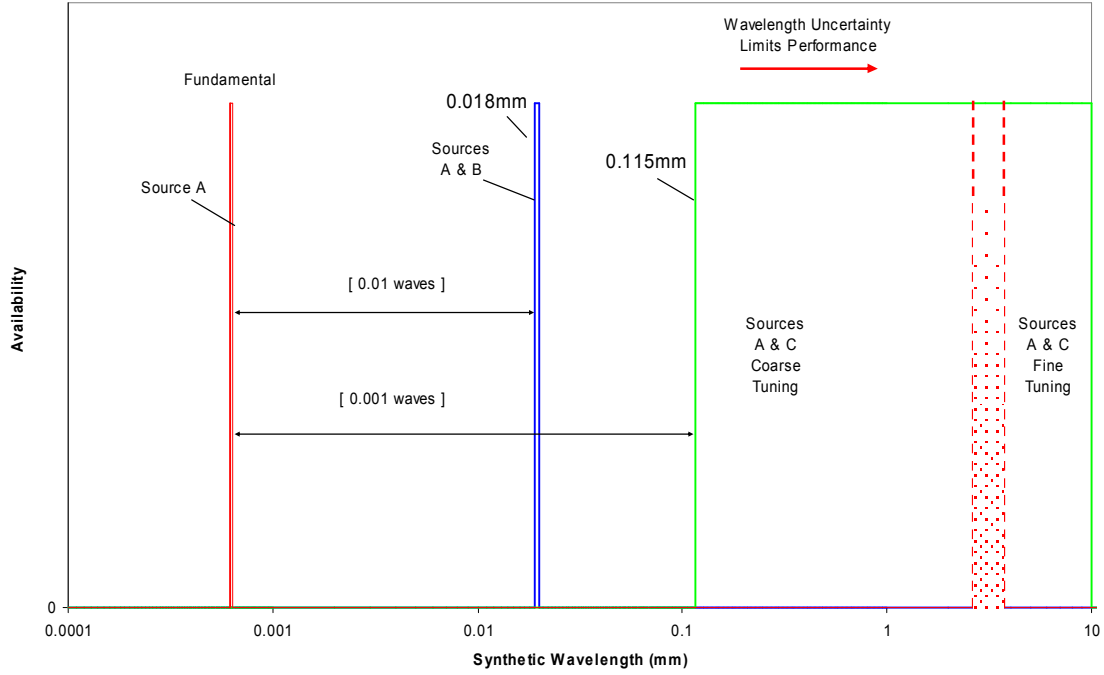
Figure 3: Synthetic wavelength coverage range (Source A = 637nm, Source B = 660nm and Source C = TLS). The precision required to jump to the fundamental wavelength is shown in [brackets].

3.2 Wavelength stability and repeatability requirements

The uncertainty of the two-wavelength measurement can be estimated by applying standard propagation of errors techniques to equation (2.1)[7]. Assuming that the wavelength uncertainty and the inherent interferometer phase errors are independent the initial estimate of the uncertainty is given by

$$u_{OPD}^2 = \left(\frac{\Delta f_s}{4p}\right)^2 \cdot u_{I_s}^2 + \left(\frac{I_s}{4p}\right)^2 \cdot u_{\Delta f_s}^2 , \tag{3.1}$$

where $u_{I_s}^2$ and $u_{\Delta f_s}^2$ are the variances in the synthetic wavelength and phase measurement respectively. The synthetic phase uncertainty can be further broken down into two components; phase independent and phase dependent. The phase independent component is fixed and is not affected by averaging. Whereas the phase dependent, or so-called print-through errors, which are present in all interferometers, are reduced by a factor of $1/\sqrt{N}$ when N measurements are averaged. In addition, the single measurement phase uncertainty can be related to the synthetic phase uncertainty by simply multiplying by two, resulting in the following relationship.

$$u_{\Delta f_s}^2 = 2 \cdot \left(u_{\Delta f_i}^2 + \frac{u_{\Delta f_d}^2}{N} \right) \tag{3.2}$$

Here $u_{\Delta f_i}^2$ represent the variance of the phase independent component and $u_{\Delta f_d}^2$ is the variance of the phase dependent component of a single wavelength measurement.

Similarly the synthetic wavelength uncertainty can be related to the uncertainty of the individual wavelengths by applying propagation of errors to the synthetic wavelength equation in (2.1). The synthetic wavelength uncertainty becomes

$$u_{I_s}^2 = \left(\frac{I_s}{I_1} - \frac{I_s^2}{I_1 \cdot I_2} \right)^2 \cdot u_{I_1}^2 + \left(\frac{I_s}{I_2} - \frac{I_s^2}{I_1 \cdot I_2} \right)^2 \cdot u_{I_2}^2$$

$$I_s \gg I_1 \quad and \quad I_s \gg I_2 \quad \therefore$$

$$u_{I_s}^2 \approx \left(\frac{I_s^2}{I_1^2} \right) \cdot \left(u_{I_1}^2 + u_{I_2}^2 \right)$$

(3.3)

Inserting equations (3.2) and (3.3) into equation (3.1) provides the final estimate for the multiple wavelength measurement uncertainty

$$U_{OPD} = K \cdot \sqrt{ \left(\frac{\Delta f_s}{4p} \right)^2 \cdot \left(\frac{I_s^4}{I_1^4} \right) \cdot \left(u_{I_1}^2 + u_I^2 \right) + 2 \cdot \left(\frac{I_s}{4p} \right)^2 \cdot \left(u_{\Delta f_i}^2 + \frac{u_{\Delta f_d}^2}{N} \right) },$$

(3.4)

where K is the coverage factor and is typically assigned a value of 2.

By detecting a heterodyne beat signal between the fixed source and the TLS before tuning to the required wavelength, the uncertainty in the TLS wavelength can be reduced from an absolute accuracy of 100pm down to a repeatability of a few picometers. The uncertainty trends in figure 3 represent the estimated measurement error when using the TLS as the second source. Since the TLS is tuned to the desired wavelength before a measurement begins, tuning the TLS and locating the heterodyne signal does not affect the acquisition time of a two-wavelength measurement.
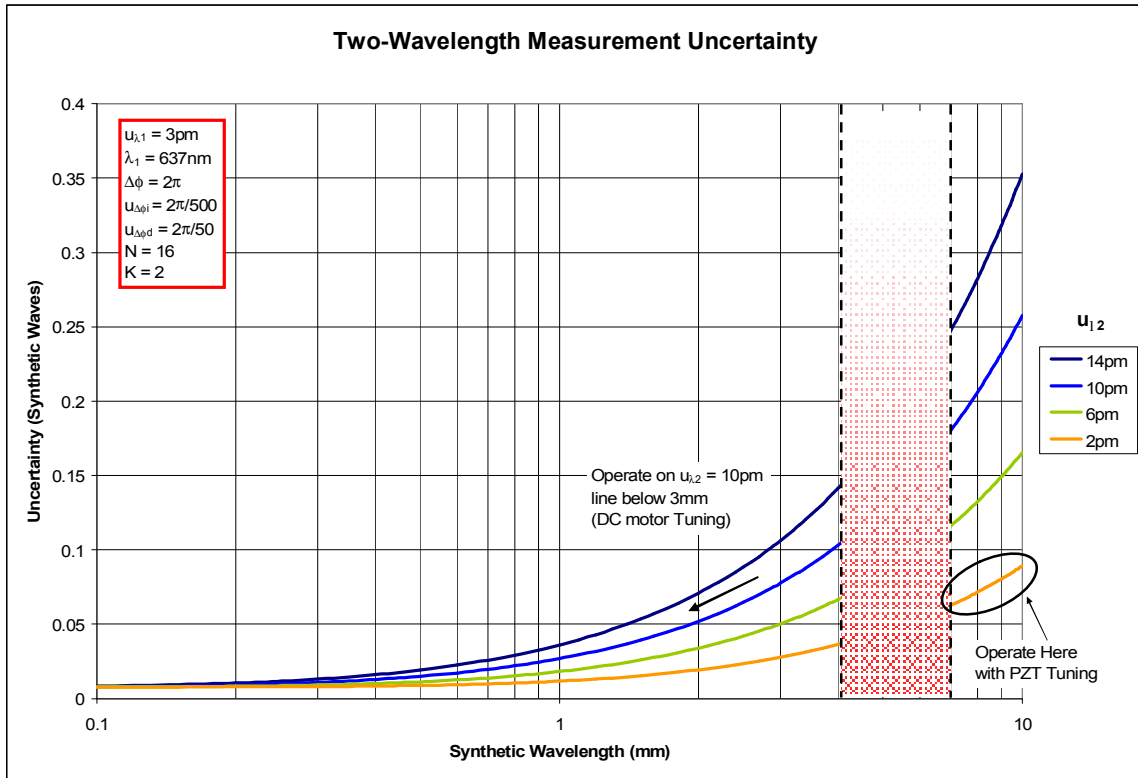

Figure 3: Two-Wavelength Measurement Uncertainty: 637nm source and TLS

For the longer synthetic wavelengths, 0.1mm to 10mm, there are two modes of operation for the TLS. For synthetic wavelengths below 7mm the grating in the laser (wavelength) is tuned using a DC motor and for synthetic wavelengths above 7mm the grating is tuned by a piezo-electric transducer. The DC motor offers a larger range of wavelength tuning and the PZT provides higher relative wavelength accuracy.

It is clear that the accuracy of a single measurement using a synthetic wavelength of 10mm is not sufficient to measure the height of a discontinuity down to the nanometer level. It takes a series of measurements at different synthetic wavelengths to achieve accuracies of a few nanometers. Measurements at longer synthetic wavelengths are used to correct the modulo $2p$ phase ambiguities at shorter wavelengths. By choosing the appropriate wavelengths it is possible to correct the phase ambiguities all the way down to the fundamental wavelength thus providing the accuracy of a single wavelength measurement.

Figure 4 shows the estimated uncertainty trends when two fixed sources are used and the heterodyne signal is not available. The uncertainties are plotted in fundamental wavelengths (637nm) in order to predict how well the two-wavelength measurement can correct phase ambiguities of measurements obtained using the fundamental wavelength. The requirement for correcting the phase ambiguities is that the measurement uncertainty at the synthetic wavelength must be below half the fundamental wavelength. At the shorter synthetic wavelengths, it is the inherent phase uncertainties of the interferometer rather than the wavelength uncertainty of the sources that generally limits the performance.
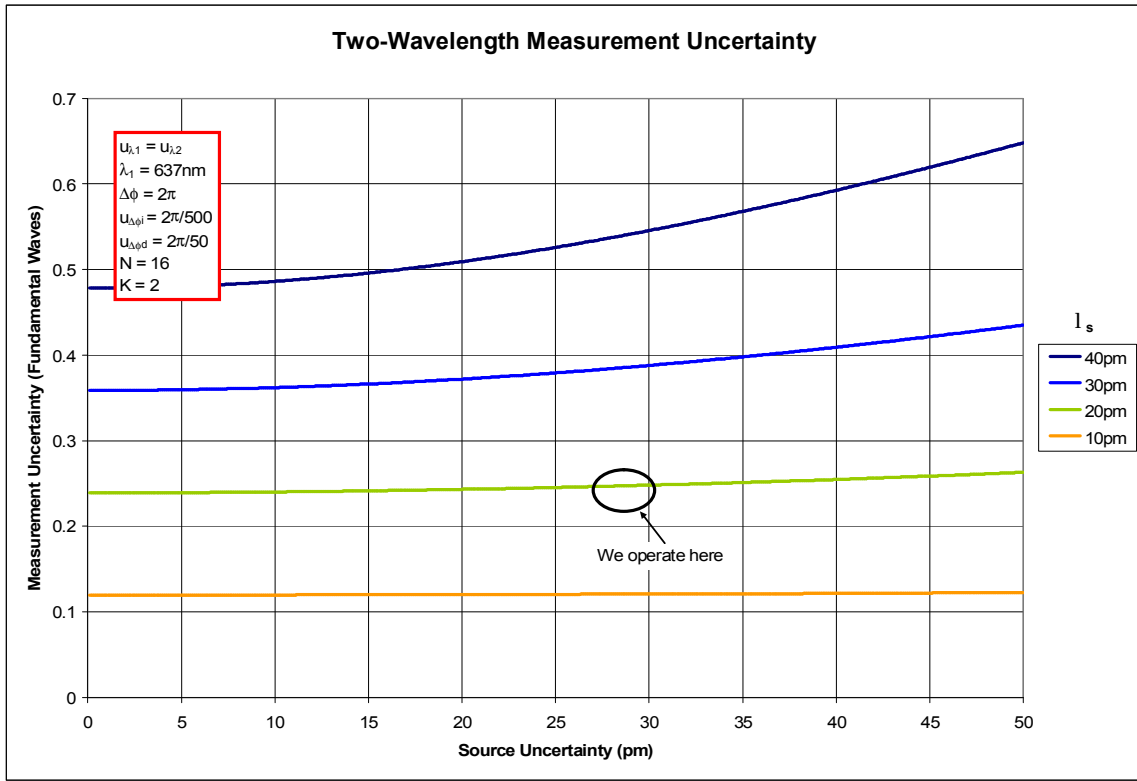

Figure 4: two-wavelength measurement uncertainty trends: 637nm source and 660nm source

4. FREQUENCY RESPONSE

Dynamic interferometry implies the ability to make measurements in the presence of vibrations. The combination of spatial phase-shifting, relatively efficient coupling of the sources into the optical path and high speed switching qualifies this interferometer as dynamic. The total acquisition time for the two-wavelength measurement is less than 100µs, over three orders of magnitude shorter than conventional interferometers.

There are two figures of merit for the dynamic performance of the multiple-wavelength interferometer; fringe contrast and how much the phase changes between the two individual measurements in the presence of vibrations. The fringe contrast limited frequency response can be estimated by examining the fringe contrast reduction for a single wavelength

measurement in the presence of a single vibrational frequency, f. The condition for good fringe contrast is expressed mathematically as follows

$$\frac{8 \cdot p}{l_1} \cdot A \cdot Sin(p \cdot t \cdot f) \square\ 2 \cdot p$$

and

$$t << \frac{1}{f}$$

(4.1)

,

where A is the radial amplitude of the vibration, t is the integration time of a single frame and l is the wavelength of light. Integrating the fringe pattern over the integration time using the time dependent phase expression in (4.1) and calculating the fringe contrast leads to the following expression for the fringe contrast.

$$V = Sinc\left(\frac{4 \cdot A \cdot p^2 \cdot t \cdot f}{l_1}\right),$$

(4.2)

Figure 5 shows the frequency response when the contrast reduction is limited to 50%. The sloping segment of the line is the region where the fringe contrast is reduced due to phase changes during the integration time as described by equation (4.2), the plateau below 2 Hz represents a fringe contrast reduction due to the fringe density on the CCD and the cutoff at 5KHz represents a reduction in fringe contrast resulting from the integration time approaching the period of the vibration.
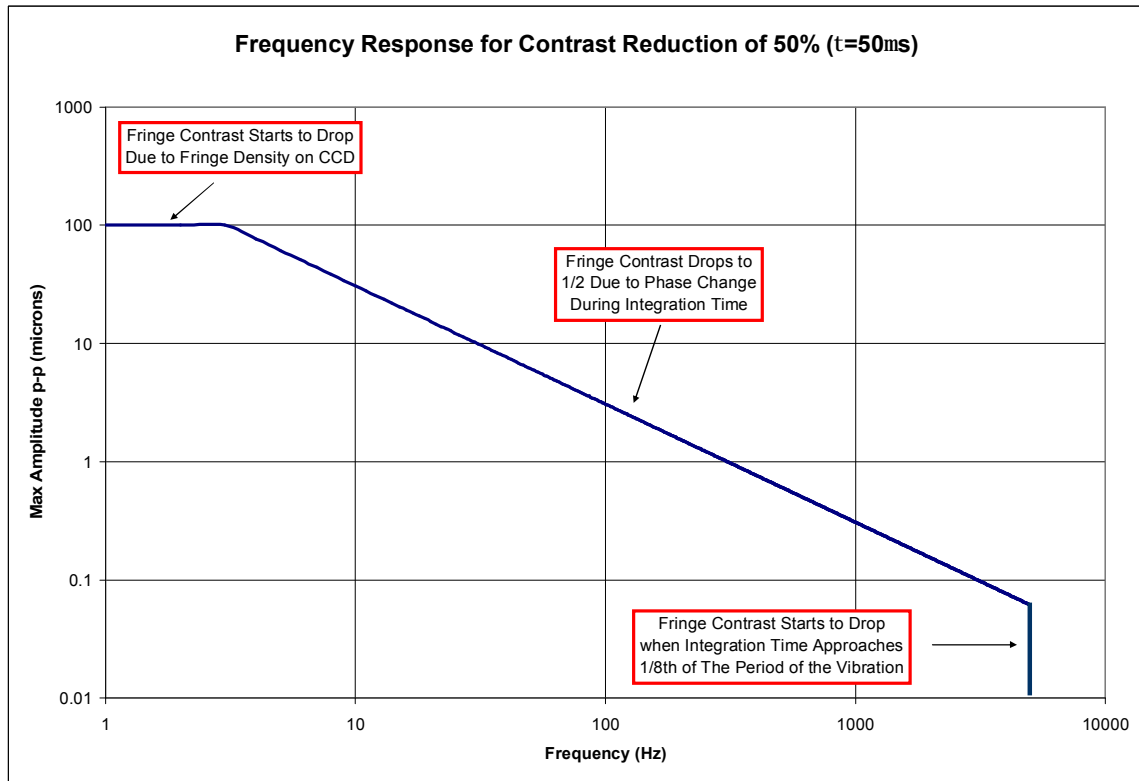

Figure 5: Fringe contrast limited frequency response

The second figure of merit is how much does the phase change between the two single wavelength measurements and what is the error that results. There are two measurement conditions that need to be examined to answer this question: 1) the mirror under test moves as a monolith, that is, the segments do not change their relative position and there is no perturbation of the surface shape due to the vibration, 2) the segments move relative to one another. For the first case the

phase change between frames leads to tilt and piston changes in the two-wavelength measurement which, are typically subtracted from interferometric measurements. As a result, the frequency response is limited by the fringe contrast as described above.

For the case of the segments moving relative to one another there will be a decided difference between the two-wavelength measurement and the instantaneous state of the surface. The simplest way to estimate the frequency response is to limit the phase change between the two single wavelength measurements. Figure 6 shows the phase change limited frequency response when the phase change between frames is restricted to $1/10^{th}$ wave.
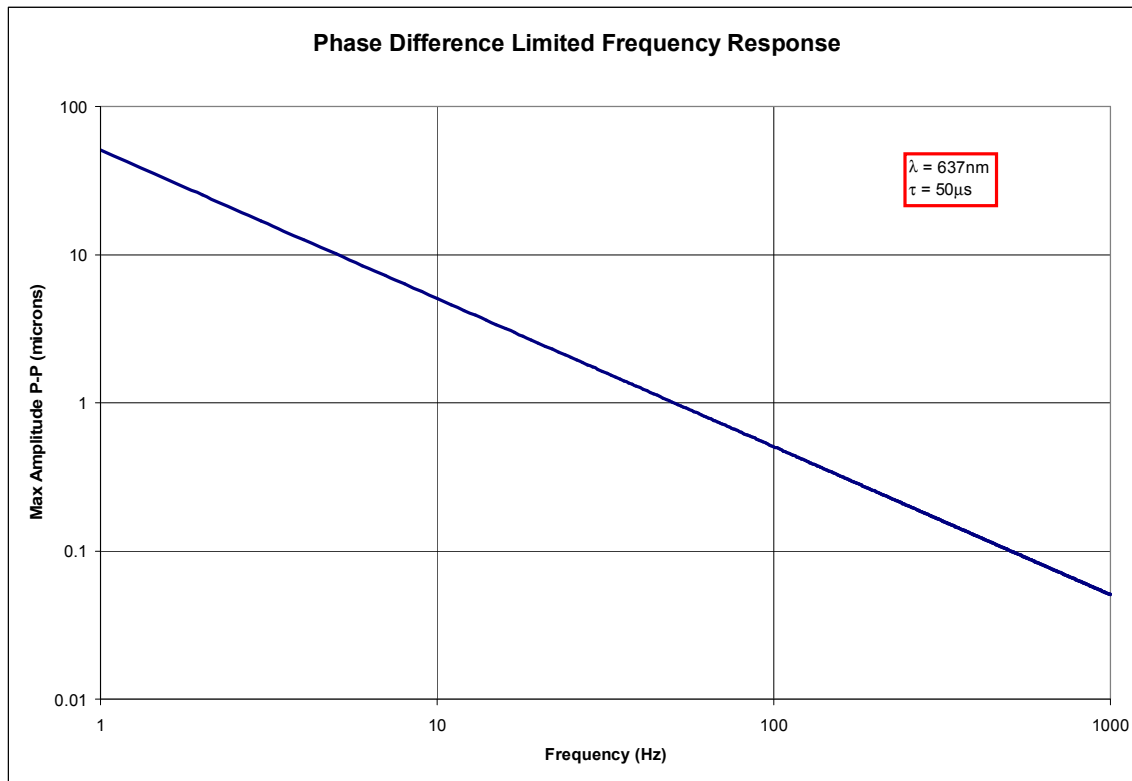
Phase Difference Limited Frequency Response

Figure 6: Frequency Response Due to Non-common Mode Vibrations: Phase change between frames is restricted to $1/10^{th}$ wave

5. RESULTS

To assess the performance of the multiple-wavelength interferometer presented in this paper three measurements were made. The first was a measurement of a step standard using a synthetic wavelength of 10mm. The step standard was constructed by wringing four gauge blocks to an optical flat as shown in figure 7. The uncertainty of the relative height between the gauge blocks wrung in this fashion was on the order of 1nm. By comparing the measured step heights with the theoretical values an estimate of the performance of the interferometer was obtained. The remaining two measurements were single wavelength measurements of an optical flat at 637nm and 660nm. Analyzing the single wavelength performance of the interferometer at the two extremes of the wavelength range demonstrated the achromatic nature of the pixelated spatial phase-shifting approach.
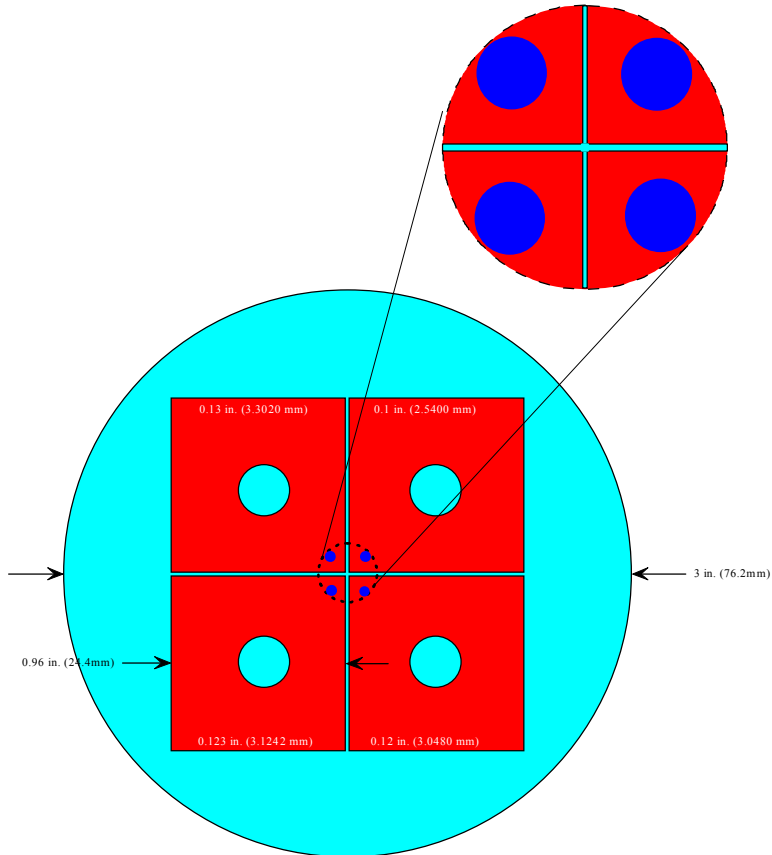
Figure 7: Calibration Step Standard; Four gauge blocks wrung to an optical flat

Figure 8 shows the result of the step standard measurement. For this measurement 16 sets of data were averaged together and the step heights were estimated by finding the mean height in each of the masked regions. The three largest steps were used to estimate the performance. Before taking the measurement, the relative tuning of the TLS was calibrated using the step standard. The resulting measurement is an estimate of the residual errors in the step height measurement. Since it is most susceptible to wavelength errors, a synthetic wavelength of 10mm was chosen for the two-wavelength performance analysis. The average offset of the step height measurements was less than 2.5 milliwaves.

To determine the instrument repeatability at the two extremes of the wavelength range a series of measurements was obtained. 10 measurements were made of the test mirror, each consisting of 16 averages. The results of the study are shown in table 1. The uncalibrated accuracy, defined as the average over all 160 measurements was well below 1/100th wave rms at both wavelengths. Precision, defined as the average deviation of each measurement from the average over all 160 measurements, was below 1/500th wave rms at both wavelengths. Finally, the repeatability, defined as the standard deviation of the 10 measurements was below ½ milliwave rms at both wavelengths. The single wavelength performance statistics indicate that there is no noticeable difference in the interferometer performance over the wavelength range of operation.
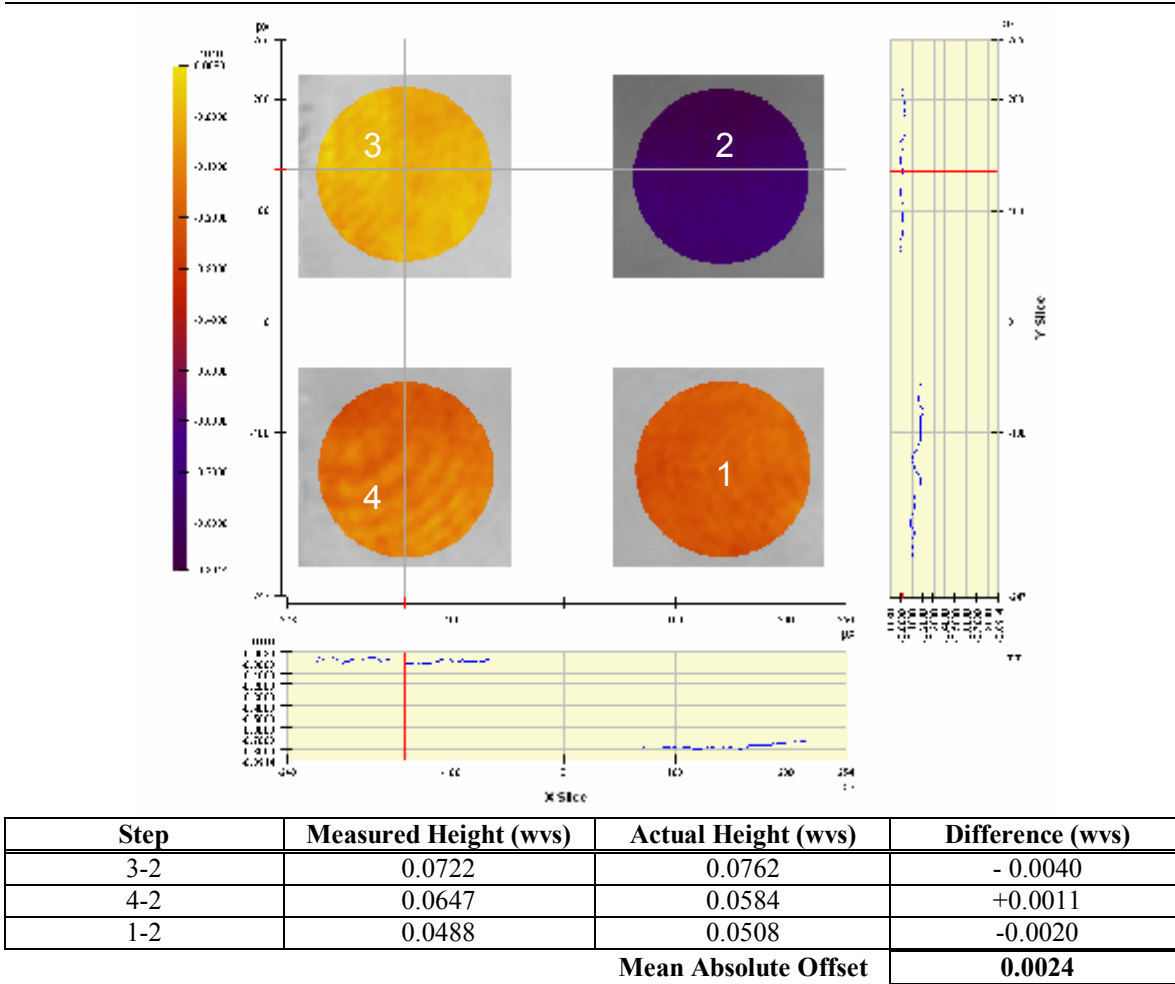
Step	Measured Height (wvs)	Actual Height (wvs)	Difference (wvs)
3-2	0.0722	0.0762	- 0.0040
4-2	0.0647	0.0584	+0.0011
1-2	0.0488	0.0508	-0.0020
		Mean Absolute Offset	**0.0024**

Figure 8: Measurement of step standard using a synthetic wavelength of 10mm

	637nm	660nm
Uncalibrated Accuracy	0.0081 waves rms	0.0079 waves rms
Precision	0.0014 waves rms	0.0010 waves rms
Repeatability	0.0002 waves rms	0.0004 waves rms

Table 1: Measured performance of the single wavelength performance at the extremes of the wavelength range.

5. CONCLUSION

We have demonstrated a new dynamic phase-shifting multi-wavelength interferometer that takes advantage of achromatic pixelated spatial phase-shifting to reduce the required acquisition time without introducing wavelength dependent errors. The interferometer is has a total acquisition time of less than 100 microseconds making it largely insensitive to vibrations. In addition, multiple wavelengths are available allowing the user to select the appropriate dynamic range for their measurement requirements. We have demonstrated a multi-wavelength Twyman-Green interferometer, analyzed the measurement uncertainty and frequency response,showed excellent repeatability at the two extremes of the wavelength range and demonstrated accuracies of less than 1/50th wave at a synthetic wavelength of 10mm.

[1] Y.-Y. Cheng, J.C. Wyant "Multiple-Wavelength Phase-Shifting Interferometry" *Applied Optics* Vol. 24, No. 6, pp. 804-807, 1985.

[2] R. Smythe, R. Moore "Instantaneous phase measuring interferometry" *Optical Engr.* Vol. 23, No. 4, PP. 361, 1984.

[3] C. Koliopoulos, "Simultaneous phase shift interferometer" SPIE Vol. 1531, PP.119-127, Advanced Optical Manufacturing and Testing II, 1991.

[4] B. Barrientos et. Al. "Transient Deformation Measurement with ESPI Using a Diffractive Optical Element for Spatial Phase-Stepping" Fringe, PP.317-8, Akademie Verlag (1997)

[5] J.E. Millerd and N.J. Brock, US Patent No. 6,304,330 and 6,522,808 "Methods and apparatus for splitting imaging and measuring wavefronts in interferometry" Oct 16, 2001

[6] M. Kuchel "The new Zeiss interferometer" SPIE Vol. 1332 Optical Test and Metrology III: Recent Advances in Industrial Optical Inspection, pp. 655-663, 1990.

[7] G.L. Squires Practical Physics, Cambridge University Press, New York, 1993